https://doi.org/10.1051/itmconf/20246101014

# Distribution amplitude and decay constant of 1S and 2S state light mesons in the light-front quark model

*Muhammad Fauzan* Syahbana[1], *Ahmad Jafar* Arifi[2,3,*], and *Terry* Mart[1]

[1]Department of Physics, Faculty of Mathematics and Natural Sciences (FMIPA), Universitas Indonesia, Depok 16424, Indonesia
[2]Few-Body System in Physics Laboratory, RIKEN Nishina Center, Wako 351-0198, Japan
[3]Research Center for Nuclear Physics, Osaka University, Ibaraki, Osaka 567-0047, Japan

**Abstract.** Studying meson structures is essential for gaining insights into the nonperturbative nature of Quantum Chromodynamics (QCD). This study will focus on calculating the decay constant and distribution amplitudes (DAs) of unflavored light mesons ($\pi$ and $\rho$) in the $1S$ and $2S$ states using the Light Front Quark Model. This study utilizes the QCD-motivated Hamiltonian, taking into account both contact and smeared spin-spin interactions. The two lowest harmonic oscillator bases are employed in this work to achieve improved results for the $2S$ states. The study found the optimal mixing parameter in basis expansion coefficients to be $\theta = 10^\circ$. Light meson properties, including the mass spectrum, decay constant, and twist-2 DAs, are then predicted using model parameters fixed through the variational principle. While the contact spin-spin interaction yields poor accuracy, the results from the smeared interaction generally agree well with experimental data and other theoretical models with $f_\pi^{1S} = 130$ MeV and $f_\rho^{1S} = 210$ MeV in the mixed state. Unlike the case for the $1S$ state, it should be noted that the properties of the $2S$ state are sensitive to the mixing parameter $\theta$. In addition, we observe that the decay constant for $\rho(2S)$ is $f_\rho^{2S} = 116$ MeV. While for $\pi(2S)$ the decay constant is extremely small with the value of $f_\pi^{2S} = 0.9$ MeV, which is mainly due to the dynamical chiral symmetry breaking.

**Keywords.** LFQM, decay constant, DAs

## 1 Introduction

The Standard Model (SM) is the leading theory of particle physics, successfully explaining three of the four fundamental forces of the universe in great detail [1, 2]. However, the SM cannot fully account for charge-parity (CP) symmetry violation via weak nuclear force interactions. The study of CP violation is conducted using the Cabibbo-Kobayashi-Maskawa (CKM) matrix, which currently represents the sole source of CP violation within the SM [3, 4]. This matrix is theoretically expected to be unitary, but recent experimental measurements have indicated a deviation from unitarity [5]. This deviation may stem from the challenges associated with measuring meson decay constants, both experimentally and theoretically. Consequently, it is crucial to further investigate meson decay constants.

*Corresponding author: ahmad.arifi@riken.jp

In recent decades, the unique properties of $B$ meson decay processes have made $B$-Physics a popular research area [6]. $B$ meson decays provide valuable insights into CP violation, the measurement of the CKM matrix, and physics beyond the SM. Within these research areas, meson distribution amplitudes (DAs) play a crucial role in examining the effects of SU(3) symmetry breaking. Meson DAs are also essential for gaining insights into meson structures and hard exclusive processes in Quantum Chromodynamics (QCD) with large momentum transfers.

Numerous non-perturbative methods for calculating decay constants and distribution amplitudes (DAs) of light mesons have been developed over the years. However, the studies for the excited states of mesons remains relatively scarce, which will be the main motivation of this study. Our methodology is based on light-front dynamics (LFD), initially proposed by Paul Dirac in 1949 [7]. Unlike other forms of dynamics, LFD offers a rational form for the Hamiltonian energy, simplifying the description of the Fock state of the vacuum. This study utilizes the light-front quark model (LFQM), which is an effective model built upon LFD principles and the constituent quark picture.

## 2 Model description

In this work, we will employ LFQM formalism based on the model developed by Choi and Ji [8]. The choice of the $x^+ = t + z$ quantization plane allows for a rational energy-momentum relation. Consequently, the Fock vacuum state is simplified as vacuum fluctuations are suppressed in this formalism. The model wave function can thus be expressed as follows,

$$\Psi^{JJ_z}_{nS}(x,\boldsymbol{k}_\perp,\lambda\bar{\lambda}) = \Phi_{nS}(x,\boldsymbol{k}_\perp)\mathscr{R}^{JJ_z}_{\lambda\bar{\lambda}}(x,\boldsymbol{k}_\perp).$$

This wave function is defined in Lorentz-invariant variables: $x_i = p_i^+/P^+$, $\boldsymbol{k}_{\perp i} = \boldsymbol{p}_{\perp i} - x_i\boldsymbol{P}_\perp$, and $\lambda_i$, where $P$, $p_i$, and $\lambda_i$ represent the meson momentum, constituent quark momentum, and helicity, respectively.

The $\Phi_{nS}$ is the mixed radial wave function composed of a superposition of $1S$ and $2S$ harmonic oscillator (HO) basis functions, achieved through a mixing parameter $\theta$ as,

$$\begin{pmatrix} \Phi_{1S} \\ \Phi_{2S} \end{pmatrix} = \begin{pmatrix} \cos\theta & \sin\theta \\ -\sin\theta & \cos\theta \end{pmatrix} \begin{pmatrix} \phi^{\rm HO}_{1S} \\ \phi^{\rm HO}_{2S} \end{pmatrix},$$

where we will consider two values for $\theta$ to represent pure states with one basis function ($\theta = 0^\circ$) and mixed states with two basis functions ($\theta = 10^\circ$). The two lowest HO basis functions are given by,

$$\phi^{\rm HO}_{1S}(\boldsymbol{k}) = \frac{1}{\pi^{3/4}\beta^{3/2}} e^{-\boldsymbol{k}^2/2\beta^2}, \quad (1)$$

$$\phi^{\rm HO}_{2S}(\boldsymbol{k}) = \frac{(2k^2 - 3\beta^2)}{\sqrt{6}\pi^{3/4}\beta^{7/2}} e^{-\boldsymbol{k}^2/2\beta^2}, \quad (2)$$

where $\boldsymbol{k} = (\boldsymbol{k}_\perp, k_z)$ is the momentum of each quark and $\beta$ is the Gaussian parameter determined through variational principle. Additionally, we perform a momentum variable transformation into $\boldsymbol{k} = (\boldsymbol{k}_\perp, x)$ by using the following relation,

$$k_z = \left(x - \frac{1}{2}\right) M_0 + \frac{m^2_{\bar{q}} - m^2_q}{2M_0},$$

where we use constituent quark $m_q = m_u = m_d$ and,

$$M_0^2 = \frac{\boldsymbol{k}_\perp^2 + m_q^2}{x} + \frac{\boldsymbol{k}_\perp^2 + m_{\bar{q}}^2}{1-x},$$

such that,

$$\phi_{nS}^{\text{HO}}(x, \boldsymbol{k}_\perp) = \sqrt{2(2\pi)^3}\sqrt{\frac{\partial k_z}{\partial x}}\phi_{nS}^{\text{HO}}(\boldsymbol{k}),$$

with a Jacobian factor,

$$\frac{\partial k_z}{\partial x} = \frac{M_0}{4x(1-x)}\left[1 - \frac{(m_q^2 - m_{\bar{q}}^2)^2}{M_0^4}\right].$$

The $\mathscr{R}_{\lambda\bar{\lambda}}^{JJ_z}$ represents the spin-orbit wave function that's obtained through Melosh transformation [9]. For pseudoscalar ($J^{PC} = 0^{-+}$) and vector mesons ($J^{PC} = 1^{--}$), the covariant forms are given by,

$$\mathscr{R}_{\lambda_q\lambda_{\bar{q}}}^{00} = -\frac{1}{\sqrt{2}\tilde{M}_0}\bar{u}_{\lambda_q}(p_q)\gamma_5 v(p_{\bar{q}}),$$
$$\mathscr{R}_{\lambda_q\lambda_{\bar{q}}}^{1J_z} = -\frac{1}{\sqrt{2}\tilde{M}_0}\bar{u}_{\lambda_q}(p_q)\left[\not{\epsilon}(J_z) - \frac{\epsilon\cdot(p_q - p_{\bar{q}})}{M_0 + m_q + m_{\bar{q}}}\right]v(p_{\bar{q}}),$$

where $\tilde{M}_0 \equiv \sqrt{M_0^2 - (m_q - m_{\bar{q}})^2}$ and the polarization vectors $\epsilon^\mu(J_z)$ for vector meson is defined by,

$$\epsilon^\mu(\pm 1) = \left(0, \frac{2}{P^+}\boldsymbol{\epsilon}_\perp(\pm 1)\cdot\boldsymbol{P}_\perp, \boldsymbol{\epsilon}_\perp(\pm 1)\right)$$

for transverse polarization where,$\boldsymbol{\epsilon}_\perp(\pm 1) = \mp\frac{1}{\sqrt{2}}(1, \pm i)$ and,

$$\epsilon^\mu(0) = \frac{1}{M_0}\left(P^+, \frac{-M_0^2 + \boldsymbol{P}_\perp^2}{P^+}, \boldsymbol{P}_\perp\right)$$

for longitudinal polarization. In this form, the spin-orbit wave function is normalized to unity, ensuring the total wave function is also normalized.

In this work, we use the QCD-motivated Hamiltonian $H_{q\bar{q}} = H_0 + V_{q\bar{q}}$ with relativistic kinetic energy $H_0 = \sqrt{m_q^2 + \vec{k}^2} + \sqrt{m_{\bar{q}}^2 + \vec{k}^2}$. The interaction potential $V_{q\bar{q}}$ consists of linear confinement $V_{\text{Conf}} = a + br$, Coulomb $V_{\text{Coul}} = -\frac{4\alpha_s}{3r}$, and spin-spin or hyperfine potential. We should note that we use two different spin-spin potentials: firstly, the contact interaction $V_{\text{Hyp}}^{\text{contact}}$; and secondly, the smeared interaction $V_{\text{Hyp}}^{\text{smeared}}$ which are written as,

$$V_{\text{Hyp}}^{\text{contact}} = \frac{2\boldsymbol{S}_q\cdot\boldsymbol{S}_{\bar{q}}}{3m_q m_{\bar{q}}}\frac{16\pi\alpha_s}{3}\delta^3(\vec{r}),$$
$$V_{\text{Hyp}}^{\text{smeared}} = \frac{2\boldsymbol{S}_q\cdot\boldsymbol{S}_{\bar{q}}}{3m_q m_{\bar{q}}}\frac{16\pi\alpha_s}{3}\frac{\sigma^3}{\pi^{3/2}}e^{-\sigma^2\vec{r}^2}.$$

The mass eigenvalue is computed as $M_{q\bar{q}} = \langle\Psi_{q\bar{q}}|H_{q\bar{q}}|\Psi_{q\bar{q}}\rangle$. The parameters in this LFQM model are the constituent quark mass ($m_q$), Gaussian parameters ($\beta_\pi, \beta_\rho$), and potential parameters ($a, b, \alpha_s, \sigma$). We will use variational principle and fit the mass of $\pi(1S)$ and $\rho(1S)$ [5] to determine the model parameters. While, the $V_{\text{Hyp}}^{\text{contact}}$ potential is treated perturbatively, the $V_{\text{Hyp}}^{\text{smeared}}$ potential we will be treated non-perturbatively. We should note that when the contact interaction is treated non-perturbatively, it can lead to a so-called 'negative infinity problem,' where the mass of the pseudoscalar meson is not minimized. Consequently, in this work, we will consider two models: one with a perturbative contact spin-spin potential and another with a nonperturbative smeared spin-spin potential.

## 3 Decay constants and distribution amplitudes

With the obtained parameters, we will use the model wave function to calculate the meson decay constants and twist-2 DAs. The decay constants for pseudoscalar and vector mesons are defined as,

$$\langle 0|\bar{q}\gamma^{\mu}\gamma_5 q|P\rangle = i f_P P^{\mu},$$
$$\langle 0|\bar{q}\gamma^{\mu} q|V(P,\lambda)\rangle = f_V M e^{\mu}(\lambda).$$

In LFQM, the decay constant is explicitly written as,

$$f_P = 2\sqrt{6}\int_0^1 \mathrm{d}x \int \frac{\mathrm{d}^2\boldsymbol{k}_\perp}{2(2\pi)^3}\frac{\Phi(x,\boldsymbol{k}_\perp)}{\sqrt{\mathscr{A}^2+\boldsymbol{k}_\perp^2}}\mathscr{A},$$
$$f_V = 2\sqrt{6}\int_0^1 \mathrm{d}x \int \frac{\mathrm{d}^2\boldsymbol{k}_\perp}{2(2\pi)^3}\frac{\Phi(x,\boldsymbol{k}_\perp)}{\sqrt{\mathscr{A}^2+\boldsymbol{k}_\perp^2}}\left[\mathscr{A}+\frac{2\boldsymbol{k}_\perp^2}{M_0+m_q+m_{\bar{q}}}\right],$$

where $\mathscr{A} = (1-x)m_q + x m_{\bar{q}}$.

Twist-2 DAs of mesons are defined as the probabilities of finding a meson in a state with a certain momentum fraction distribution for each parton at a small transverse separation $\mu$. Although we cannot observe DA directly from experiments, we can see its properties constrained through meson electromagnetic form factors and meson production processes. DAs can be extracted by integrating the meson wave function $\Psi_{nS}^{JJ_z}(x,\boldsymbol{k}_\perp,\lambda\bar{\lambda})$ with respect to its transverse momentum, resulting in a wave function that depends on the fractional momentum $x$,

$$\phi(x_i,\mu) = \int^{|\boldsymbol{k}_\perp|<\mu} \frac{\mathrm{d}^2\boldsymbol{k}_\perp}{2(2\pi)^3}\Psi_{nS}(x_i,\boldsymbol{k}_{\perp i}).$$

The shape of meson DA will also be constrained by its decay constant,

$$\int_0^1 \phi_{P(V)}^{\text{tw-2}}(x,\mu)\,\mathrm{d}x = \frac{f_{P(V)}^{+}}{2\sqrt{6}}.$$

We can redefine DAs $\phi_{P(V)}^{\text{tw-2}} = \frac{f_{P(V)}^{+}}{2\sqrt{6}}\tilde{\phi}_{P(V)}^{\text{tw-2}}$ so it will be normalized to unity. We can also write DAs as an expansion of Gegenabuer polynomials $C_n^{\frac{3}{2}}$ as,

$$\tilde{\phi}(x,\mu) = \tilde{\phi}_{as}(x)\left[1+\sum_{n=1}^{\infty} a_n(\mu) C_n^{\frac{3}{2}}(2x-1)\right],$$

where $a_n(\mu)$ is the Gegenbauer moment and $\tilde{\phi}_{as} = 6x(1-x)$ is the asymptotic DA. The $a_n(\mu)$ describes how much the meson DA deviate from the asymptotic one. We can also define $\xi$-moment as,

$$\langle \xi^n \rangle = \int_0^1 \mathrm{d}x\ \xi^n \tilde{\phi}_{P(V)}^{\text{tw-2}}(x,\mu)$$

with $\xi = x-(1-x) = 2x-1$.

## 4 Results and discussion

Let us first discuss the model parameter that we obtained through the variational analysis. As we can see in Table 1, different fitting procedure would result in different parameters for each model with their respective mixing angle $\theta$ of the basis expansion coefficients. Only the smeared model will have the value of smearing parameter $\sigma$, while the model with contact interaction has the same Gaussian parameter $\beta$ for both mesons because we treat the hyperfine potential perturbatively.

**Table. 1.** Model parameters obtained by using variational principle and fitting the mass of $\pi(1S)$ and $\rho(1S)$.

| Model | $\theta$ | $m_q$ | $b$ | $\sigma$ | $a$ | $\alpha_s$ | $\beta_\pi$ | $\beta_\rho$ |
|---|---|---|---|---|---|---|---|---|
| Contact | $0^\circ$ | 0.22 | 0.18 | $\dots$ | $-0.723$ | 0.312 | 0.366 | |
| | $10^\circ$ | | | | $-0.724$ | 0.327 | 0.320 | |
| Smeared | $0^\circ$ | 0.18 | 0.18 | 0.42 | $-0.606$ | 0.362 | 0.614 | 0.318 |
| | $10^\circ$ | | | | $-0.608$ | 0.366 | 0.537 | 0.276 |

The computed mass spectra in the this work are presented in Table 2. We note that only mass spectra of $2S$ states are our predictions as we use the measured mass of $1S$ states as input parameters. These predictions are compared to the known experimental results for light meson masses from PDG [5]. It is evident that our results for the perturbative contact interaction yield inaccurate outcomes for the $2S$ states in both the $\theta = 0^\circ$ and $\theta = 10^\circ$ cases, with discrepancies of up to 37 %. However, in the case of the nonperturbative smeared interaction, our results are significantly more accurate, deviating from experimental data by only around 5 %.

**Table. 2.** Mass spectra of $\pi$ and $\rho$ meson (MeV) in the $1S$ and $2S$ states.

| Model | $\theta$ | $M_\pi^{1S}$ | $M_\pi^{2S}$ | $M_\rho^{1S}$ | $M_\rho^{1S}$ |
|---|---|---|---|---|---|
| Contact | $0^\circ$ | 135 | 591 | 770 | 1544 |
| | $10^\circ$ | 135 | 943 | 770 | 1415 |
| Smeared | $0^\circ$ | 135 | 1307 | 770 | 1434 |
| | $10^\circ$ | 135 | 1210 | 770 | 1456 |
| Exp [5] | | 134.97 | 1300(100) | 770 | 1465(25) |

The predictions of the decay constants are given in Table 3. We compared our prediction with the experimental data (Only for $1S$ state) and other theoretical models such as LFQM [8], RQM[10], Lattice [11–13], EHM [14], RCQ [15], QCD sum rule [16], and ECQM [17]. Similar to the case of mass spectra, the model with perturbative contact interaction gives inaccurate results, with a deviation from the data up to 37%. For the model with smeared interaction, our results for $1S$ states are within 5% errors compared to the experimental data, while the the $2S$ state our results are in good agreement with most of other theoretical models. Furthermore, the results are even better when we use the mixed state at $\theta = 10^\circ$. Here we found something interesting, the decay constant of $\pi(2S)$ is significantly smaller than the decay constant of $\pi(1S)$. Based on the QCD sum rule, the decay constant of $\pi(2S)$ will be zero in the chiral limit. A similar result is found from a Lattice QCD study as well [21]. Such a vanishing decay constant was not observed for the case of heavy mesons [18]. It shows that there is a suppression for decay constant of the excited $\pi$ meson, and will be an important constraint of the structure of light mesons.

**Table. 3.** Mass spectra of $\pi$ and $\rho$ meson (MeV) in the 1$S$ and 2$S$ states.

| Model (1$S$) | $\theta$ | $f_\pi^{1S}$ | $f_\rho^{1S}$ | Model (2$S$) | $f_\pi^{2S}$ | $f_\rho^{2S}$ |
|---|---|---|---|---|---|---|
| Contact | 0° | 130 | 246 | | 43.5 | 197 |
| | 10° | 129 | 242 | | 24.5 | 135 |
| Smeared | 0° | 131 | 214 | | 20.8 | 170 |
| | 10° | 130 | 210 | | 0.9 | 116 |
| Exp [5] | | 130.3(0.3) | 210(4) | EHM [14] | 1.1 | 38.2 |
| LFQM [8] | | 130 | 246 | RCQ [15] | 26.3 | 128 |
| RQM [10] | | 124 | 219 | Sum rule [16] | 2.20 | ... |
| Lattice [11–13] | | 126.6 | 239.4 | ECQM [17] | 0.52-2.26 | ... |

Figures 1 and 2 show the predicted DAs for $\pi$ and $\rho$ mesons, respectively. The results for 1$S$ and 2$S$ states are given in the left and right panel of each figure. Here we only show the result for the nonperturbative smeared interaction since the model provides the most accurate prediction for both mass spectra and decay constants. We present the results for pure ($\theta = 0°$) and mixed ($\theta = 10°$) states, as well as the asymptotic form of DA. It is clearly shown that the DA is symmetric along $x = 0.5$ axis, reflecting isospin symmetry of the pion. The pion DA looks more broader than the asymptotic DA, while rho meson DA is narrower and closer to the asymptotic one. This difference will be correlated to the electromagnetic form factor for each meson [19]. The DA for $\pi(2S)$ with $\theta = 10°$ is found to have extremely high peak near both endpoints and a deep valley at $x = 0.5$. The shape is completely different from those with $\theta = 10°$ as shown in the right panel of Fig. 1. Such a structure is plausibly coming from the dynamical chiral symmetry breaking (DCSB) and resulted in such low value of the decay constant of $\pi(2S)$ [20]. Table 4 shows the calculation results for Gegenabuer and $\xi$-moments. We can see immediately that the odd moments are zero from isospin symmetry, and these results correspond to the symmetric shape of the DAs. Furthermore, the $\pi(2S)$ state

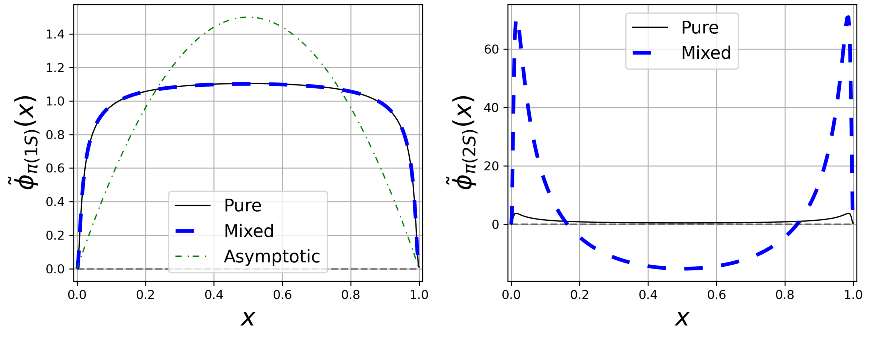


**Fig. 1.** Twist-2 DAs of $\pi(1S)$ and $\pi(2S)$ obtained with the nonperturbative smeared interaction for the case of $\theta = 0°$ and $\theta = 10°$.

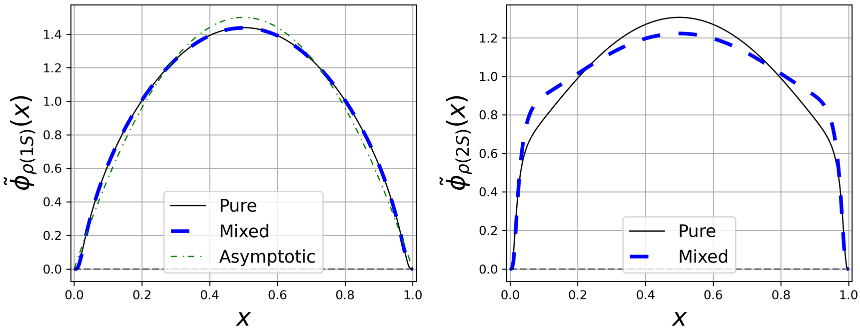


**Fig. 2.** Twist-2 DAs of $\rho(1S)$ and $\rho(2S)$ obtained with the nonperturbative smeared interaction for the case of $\theta = 0°$ and $\theta = 10°$.

results for both moments are significantly higher than other states, which is due to the high peaks of $\pi(2S)$ DA.

**Table. 4.** (Left) Gegenbauer $a_n(\mu)$ and (Right) $\xi$-moments up to $n = 6$ for $\pi$ and $\rho$ mesons in the 1$S$ and 2$S$ states with $\theta = 10°$.

| $n$ | $\pi(1S)$ | $\pi(2S)$ | $\rho(1S)$ | $\rho(2S)$ |
|---|---|---|---|---|
| 1 | ... | ... | ... | ... |
| 2 | 0.265 | 17.458 | 0.138 | 1.275 |
| 3 | ... | ... | ... | ... |
| 4 | 0.101 | 15.262 | 0.003 | 0.540 |
| 5 | ... | ... | ... | ... |
| 6 | 0.037 | 10.842 | −0.021 | 0.092 |

| $n$ | $\pi(1S)$ | $\pi(2S)$ | $\rho(1S)$ | $\rho(2S)$ |
|---|---|---|---|---|
| 1 | ... | ... | ... | ... |
| 2 | 0.291 | 6.186 | 0.247 | 0.637 |
| 3 | ... | ... | ... | ... |
| 4 | 0.157 | 5.662 | 0.118 | 0.433 |
| 5 | ... | ... | ... | ... |
| 6 | 0.102 | 4.921 | 0.069 | 0.314 |

## 5 Conclusion

In this study, we employed the Light-Front Quark Model (LFQM) with the two lowest harmonic oscillator basis functions and a QCD-motivated Hamiltonian to estimate the decay constants and distribution amplitudes (DAs) of unflavored light mesons ($\pi$ and $\rho$) in the 1$S$ and 2$S$ states. Additionally, we considered both perturbative contact and non-perturbative smeared hyperfine potentials and studied the effect to the observables.

We have found that the model with contact hyperfine potential is not accurate to explain the properties of 1$S$ or 2$S$ state light mesons when compared the predictions to experimental data and other theoretical models. On the other hand, the model with smeared hyperfine potential gives much better agreement with the experimental data. We emphasize that the mixing angle of $\theta = 10°$ is crucial to get a consistent results with other theoretical models. It is worth noting that the small value of $\pi(2S)$ decay constant may be influenced by DCSB. Such a suppression in the decay constant also gives rise to the high peaks of pion DAs and large value of Gegenbauer and $\xi$-moments. On the other hand, we have also found that the 2$S$ states are more sensitive to the change in the mixing parameter $\theta$.

For further study, we would like to explore the DCSB effects on pion decay constant alongside the decay constant and DA for other light mesons that contain strange quark to study the effect of SU(3) flavor symmetry breaking. We can explore those ideas by substituting other expressions for the meson wave function, such as the Gaussian Expansion Method (GEM) or the power law model, or by utilizing other forms of the model Hamiltonian. We could also explore to extract electromagnetic form factors from the meson DA in the excited state with the obtained light-front wave function. It is also interesting to extend the calculation for higher twist DAs [22].

## Acknowledgements

The work of A.J.A. is supported by the RIKEN special postdoctoral researcher (SPDR) program. The work of T.M. is supported by the PUTI Q2 grant from Universitas Indonesia, under contract No. NKB-663/UN2.RST/HKP.05.00/2022. The work of M.F.S is supported by Universitas Indonesia undergraduate program.

## References

1. M. K. Gaillard, P. D. Grannis, F. J. Sciulli. Rev. Mod. Phys. **71**, S96 (1999).
2. T. W. Kibble, Eur. Rev. **23**, 36 (2015).
3. M. Kobayashi and T. Maskawa, Prog. Theor. Phys. **49**, 652 (1973).
4. N. Cabibbo, Phys. Rev. Lett. **10**, 531 (1963).
5. R. L. Workman *et al.*, PTEP **2022**, 083C01 (2022).
6. R. Aaij *et al.*, Phys. Rev. Lett. **126**, 122002 (2021).
7. P. A. M. Dirac, Rev. Mod. Phys. **21**, 392 (1949).
8. H. M. Choi and C. R. Ji, Phys. Rev. D **75**, 034019 (2007).
9. H. J. Melosh, Phys. Rev. D **9**, 1095 (1974).
10. D. Ebert, R. N. Faustov, and V. O. Galkin. Phys. Lett. B **635**, 93 (2006).
11. A. A. Khan *et al.*, Phys. Rev. D **64**, 054504 (2001).
12. A. A. Khan *et al.*, Phys. Rev. D **65**, 054505 (2002).
13. A. A. Khan *et al.*, Phys. Rev. D **67**, 059901 (2003).
14. Z. N. Xu, Z. Q. Yao, S. X. Qin, Z. F. Cui, and C. D. Roberts, Eur. Phys. J. A **59**, 39 (2023).
15. D. Arndt and C. R. Ji, Phys. Rev. D **60**, 094020 (1999).
16. K. Maltman and J. Kambor, Phys. Rev. D **65**, 074013 (2002).
17. A. A. Andrianov, D. Espiru, and R. Tarrach, Nucl. Phys. B **533**, 429 (1998).
18. A. J. Arifi, H. M. Choi, and C. R. Ji, Phys. Rev. D **106**, 014009 (2022).
19. H. M. Choi and C. R. Ji, Phys. Rev. D **74**, 093010 (2006).
20. B. L. Li *et al.*, Phys. Rev. D **93**, 114033 (2016).
21. C. McNeile and C. Michael Phys. Rev. B **642**, 244 (2006).
22. A. J. Arifi, H. -M. Choi, and C. -R. Ji, Phys. Rev. D **108**, 013006 (2023).